iScience

CellPress
OPEN ACCESS

Article

Humoral immune responses against SARS-CoV-2 Spike variants after mRNA vaccination in solid organ transplant recipients

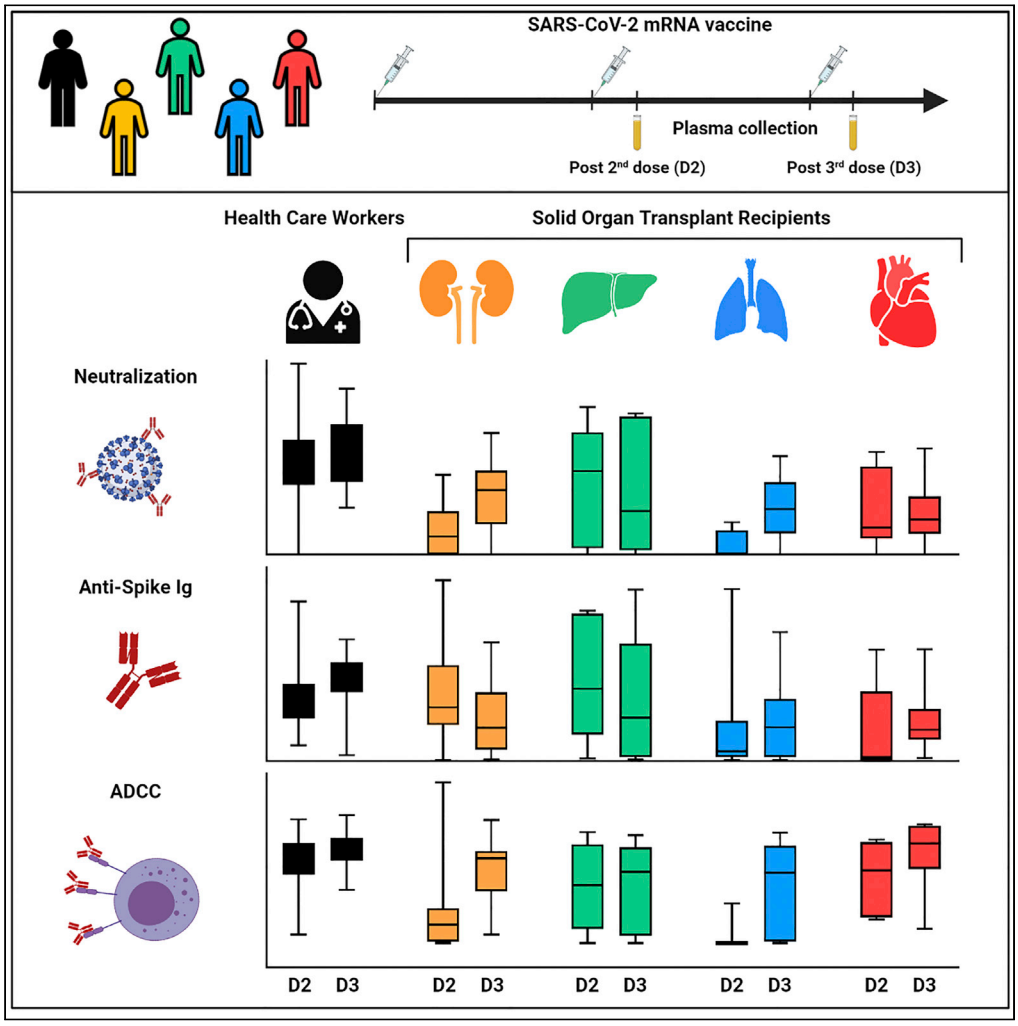

Alexandra Tauzin, Guillaume Beaudoin-Bussières, Shang Yu Gong, ..., Mélanie Dieudé, Marie-Josée Hébert, Andrés Finzi

marie-josee.hebert@umontreal.ca (M.-J.H.)
andres.finzi@umontreal.ca (A.F.)

Highlights

Two doses of mRNA vaccine elicit weak humoral responses in transplant recipients

A boost increases these responses, but below those of the general population

Robust Fc effector functions but weak neutralization is observed after the boost

Neutralizing activity is particularly poor against variants of concern

Tauzin et al., iScience 25, 104990
September 16, 2022
https://doi.org/10.1016/j.isci.2022.104990

iScience

CellPress
OPEN ACCESS

Article

Humoral immune responses against SARS-CoV-2 Spike variants after mRNA vaccination in solid organ transplant recipients

Alexandra Tauzin,[1,2] Guillaume Beaudoin-Bussières,[1,2] Shang Yu Gong,[1,3] Debashree Chatterjee,[1] Gabrielle Gendron-Lepage,[1] Catherine Bourassa,[1] Guillaume Goyette,[1] Normand Racine,[4] Zineb Khrifi,[1] Julie Turgeon,[1,5] Cécile Tremblay,[1,2] Valérie Martel-Laferrière,[1,2] Daniel E. Kaufmann,[1,6] Héloïse Cardinal,[1,2,5] Marc Cloutier,[7] Renée Bazin,[7] Ralf Duerr,[8] Mélanie Dieudé,[1,2,5,7] Marie-Josée Hébert,[1,5,6,*] and Andrés Finzi[1,2,3,9,*]

SUMMARY

Although SARS-CoV-2 mRNA vaccination has been shown to be safe and effective in the general population, immunocompromised solid organ transplant recipients (SOTRs) were reported to have impaired immune responses after one or two doses of vaccine. In this study, we examined humoral responses induced after the second and the third dose of mRNA vaccine in different SOTR (kidney, liver, lung, and heart). Compared to a cohort of SARS-CoV-2 naïve immunocompetent health care workers (HCWs), the second dose induced weak humoral responses in SOTRs, except for the liver recipients. The third dose boosted these responses but they did not reach the same level as in HCW. Interestingly, although the neutralizing activity against Delta and Omicron variants remained very low after the third dose, Fc-mediated effector functions in SOTR reached similar levels as in the HCW cohort. Whether these responses will suffice to protect SOTR from severe outcome remains to be determined.

INTRODUCTION

The severe acute respiratory syndrome coronavirus 2 (SARS-CoV-2) is the etiologic agent of the coronavirus disease 2019 (COVID-19) responsible of the current pandemic. COVID-19 causes a plethora of symptoms with different degrees of severity (Sheikhi et al., 2020). In solid organ transplant recipients (SOTRs), because of immunosuppressive treatments, SARS-CoV-2 infection leads to a high rate of severe COVID-19 (Danziger-Isakov et al., 2021; Pereira et al., 2020) and therefore vaccination is strongly recommended (AST, 2022; CST, 2022). The Pfizer/BioNTech BNT162b2 and Moderna mRNA-1273 mRNA vaccines have shown a remarkable efficacy in the general population, particularly against severe outcomes (Baden et al., 2021; Polack et al., 2020). However, in SOTR, immune responses induced by vaccination are generally reduced (Kumar et al., 2011; Stucchi et al., 2018) and recent studies have shown that SOTR have impaired humoral responses after two doses of the SARS-CoV-2 mRNA vaccine (Caillard et al., 2021; Miele et al., 2021; Rabinowich et al., 2021; Rincon-Arevalo et al., 2021; Stumpf et al., 2021).

Moreover, SARS-CoV-2 is constantly evolving, and the Wuhan original strain has now been replaced by several variants. Among current circulating strains, the Delta and Omicron variants of concern (VOCs) have accumulated numerous mutations in their genome, and notably in the Spike (S) glycoprotein (Kumar et al., 2022). These VOCs are transmitted more efficiently than the original Wuhan strain and less well controlled by vaccination (Kumar et al., 2022; Lauring et al., 2022; Tseng et al., 2022). The administration of a third dose of mRNA vaccine (boost) leads to strong humoral responses and protects from severe outcome caused by these VOCs in the general population (Ariën et al., 2022; Tauzin et al., 2022a; Yoon et al., 2022). However, humoral responses elicited by the third dose on populations with compromised immune responses, particularly SOTR, are less documented. Here, we evaluated humoral responses induced in different groups of SOTR (kidney, liver, lung, and heart) after the second and third doses of the mRNA vaccine.

[1]Centre de Recherche du CHUM, Montreal, QC H2X 0A9, Canada

[2]Département de Microbiologie, Infectiologie et Immunologie, Université de Montréal, Montreal, QC H2X 0A9, Canada

[3]Department of Microbiology and Immunology, McGill University, Montreal, QC H3A 2B4, Canada

[4]Institut Cardiologie de Montréal, Montreal, QC H1T 1C8, Canada

[5]Canadian Donation and Transplantation Research Program (CDTRP), Edmonton, AL T6G 2E1, Canada

[6]Département de Médecine, Université de Montréal, Montreal, QC H3T 1J4, Canada

[7]Héma-Québec, Affaires Médicales et Innovation, Québec, QC G1V 5C3, Canada

[8]Department of Microbiology, New York University School of Medicine, New York, NY 10016, USA

[9]Lead contact

*Correspondence: marie-josee.hebert@umontreal.ca (-J.H.), andres.finzi@umontreal.ca (A.F.)

https://doi.org/10.1016/j.isci.2022.104990

RESULTS

We analyzed humoral immune responses in cohorts of 30 kidney, 10 liver, 13 lung, and 8 heart organ transplant recipients after the second (median [range]: 26 days [20–54 days]) and third doses (median [range]: 35 days [19–68 days]) of SARS-CoV-2 mRNA vaccine. The SOTR received their first two doses with different interval regimen (median [range]: 36 days [25–112 days]) and their third dose around 4 months after the second dose (median [range]: 110 days [34–195 days]), according to the province of Quebec, Canada public health authority's vaccination roll out guidelines for immunocompromised patients. Vaccine-elicited humoral responses in SOTR were compared to those measured in a cohort of SARS-CoV-2 naïve health care workers (HCWs). HCWs received their first two doses of mRNA vaccine with a 16-week extended interval (median [range]: 111 days [76–134 days]), and their third dose around seven months after the second dose (median [range]: 219 days [167–235 days]), according to the province of Quebec, Canada public health authority's vaccination roll out guidelines for HCW. Several studies have shown that this extended interval regimen leads to strong humoral and cellular responses after the second dose, notably against VOCs (Chatterjee et al., 2022; Nayrac et al., 2022; Payne et al., 2021; Tauzin et al., 2022a). This allowed us to compare humoral responses obtained in SOTR versus humoral responses elicited by a long interval vaccination regimen. Basic demographic characteristics of the cohorts, immunosuppressive treatments of the SOTR and detailed vaccination time points are summarized in Table 1 and Figures 1A and S1.

Elicitation of SARS-CoV-2 antibodies against the receptor-binding domain of the spike

We first measured anti-receptor-binding domain (RBD) IgG levels induced after the second and the third doses of the mRNA vaccine using a previously reported ELISA assay (Anand et al., 2021; Beaudoin-Bussières et al., 2020; Prévost et al., 2020; Tauzin et al., 2021). After the second dose, all HCWs presented high levels of RBD-specific IgG (Figure 1B). In contrast, in all groups of SOTR, the levels of anti-RBD antibodies (Abs) were, with the exception of liver recipients, significantly lower than in HCW. We also noted that in every SOTR group, some recipients did not have anti-RBD IgG after the second dose of mRNA vaccine. Among SOTR, liver recipients had higher Ab levels than kidney, lung, and heart recipients, in line with a generally lower immunosuppression regimen. For HCW, the third dose of the mRNA vaccine led to the same level of Abs as after the second dose, as recently described (Tauzin et al., 2022a). For SOTR, we observed a significant increase in the level of anti-RBD IgG in lung recipients and a trend for kidney and heart recipients. No increase in anti-RBD IgG level was observed for liver recipients. Of note, in all SOTR groups, anti-RBD levels remained significantly lower than in the HCW cohort even after the third dose, but the number of recipients who developed anti-RBD IgG was higher after the third than after the second dose, suggesting the initiation of an antibody response by repeated antigen exposure.

Recognition of SARS-CoV-2 spike variants and a common-cold human *Betacoronavirus*

We next evaluated the recognition of the SARS-CoV-2 full-length S after vaccination in SOTR and HCW by flow cytometry (Figure 2A). After the second vaccine dose, no significant differences were observed in the recognition of the D614G S by plasma from kidney and liver recipients and HCW. In contrast, lung and heart recipients recognized the D614G S less efficiently, although this difference was not significant for heart recipients, likely because of the low number of recipients in this group. The third dose increased the D614G S recognition for HCW, and we noted a slight increase for lung and heart recipients, for whom the recognition was very weak after the second dose. For kidney and liver recipients, the third dose did not improve the D614G S recognition (Figure 2A).

It has been well documented that Delta and Omicron VOCs are less efficiently recognized by Abs induced by vaccination, because of accumulated mutations in the S glycoproteins compared to the original Wuhan strain, used for the development of current mRNA SARS-CoV-2 vaccines (Chatterjee et al., 2022; Planas et al., 2021; Tauzin et al., 2022a). We measured the recognition of these VOCs S after mRNA vaccination in SOTR (Figures 2B and 2C). We did not see significant differences in the level of recognition of Delta and Omicron S between liver recipients and HCW after the second dose. The third dose led to a slight increase of the recognition of the VOCs S except for liver recipients, however, it remained significantly lower than in HCW. When we compared S recognition between the SARS-CoV-2 variants (Figure S2), we observed that in HCW, because of strong humoral responses induced by the extended interval, no major differences in recognition were observed between D614G and VOCs S after the second and third doses of mRNA vaccine (Figure S2A). For SOTR, VOCs S were significantly less recognized than the D614G S, suggesting that vaccination in SOTR did not improve the breadth of S recognition, as observed in HCW (Figures S2B–S2E).

Table 1. Characteristics of the SARS-CoV-2 vaccinated SOTR and HCW cohorts

			SOTR				
		HCW	Entire cohort	Kidney	Liver	Lung	Heart
Age		52 (33–64)	46 (21–82)	45 (23–73)	46 (21–59)	38 (26–59)	66 (58–82)*
Sex	Male (n)	8	37	18	6	7	6
	Female (n)	12	24	12	4	6	2
Immunosuppression	Prednisone (n)	N/A	45	30	3	12	0
	Daily dose (mg)		5 (2–20)	5 (2–20)	5 (2.5–5)	10 (5–10)	
	Tacrolimus (n)	N/A	55	27	9	13	6
	Daily dose (mg)		4 (1.5–14)	3.5 (1.5–14)	5 (2.5–10)	7 (2–10)	2.5 (1.5–7)
	Mycophenolate mofetil/	N/A	46	25	1	12	8
	mucophenolate sodium (n)		875 (100–7200)	720 (360–7200)	500	860 (100–3000)	1440 (720–1500)
	Daily dose (mg)						
	Cyclosporin (n)	N/A	2	1	0	0	1
	Daily dose (mg)		122.5 (110–135)	135			110
	Sirolimus (n)	N/A	4	2	1	0	1
	Daily dose (mg)		2.5 (1–3)	2.5 (2–3)	1		3
	Azathioprine (n)	N/A	4	1	2	1	0
	Daily dose (mg)		37.5 (25–100)	50	62.5 (25–100)	25	
Years between transplantation and the 1st dose[a]		N/A	4.66 (−0.40–36.28)	2.04 (−0.40–22.93)	3.81 (0.66–36.28)	3.67 (1.15–20.07)	11.41 (3.20–23.65)
Days between the 1st and 2nd dose[a]		111 (76–120)*	36 (25–112)	34 (28–75)	37 (28–112)	32 (25–92)	84 (62–101)*
Days between the 2nd and 3rd dose[a]		219 (167–230)*	110 (34–195)	111 (34–153)	113 (74–147)	104 (81–169)	81 (78–195)
Days between the 2nd dose and D2[a]		21 (17–34)	26 (20–54)	27 (22–45)	25 (22–35)	26 (22–28)	28 (20–54)
Days between the 3rd dose and D3[a]		27 (20–38)	35 (19–68)	35 (19–48)	35 (21–55)	41 (28–68)	30 (22–51)

[a]Values displayed are medians, with ranges in parentheses. Continuous variables were compared by using Kruskal-Wallis tests. $p < 0.05$ was considered statistically significant for all analyses. Statistical differences were found for the age of heart recipients, the interval between the first and second doses of the HCW and heart recipients, the interval between the second and third doses of the HCW.

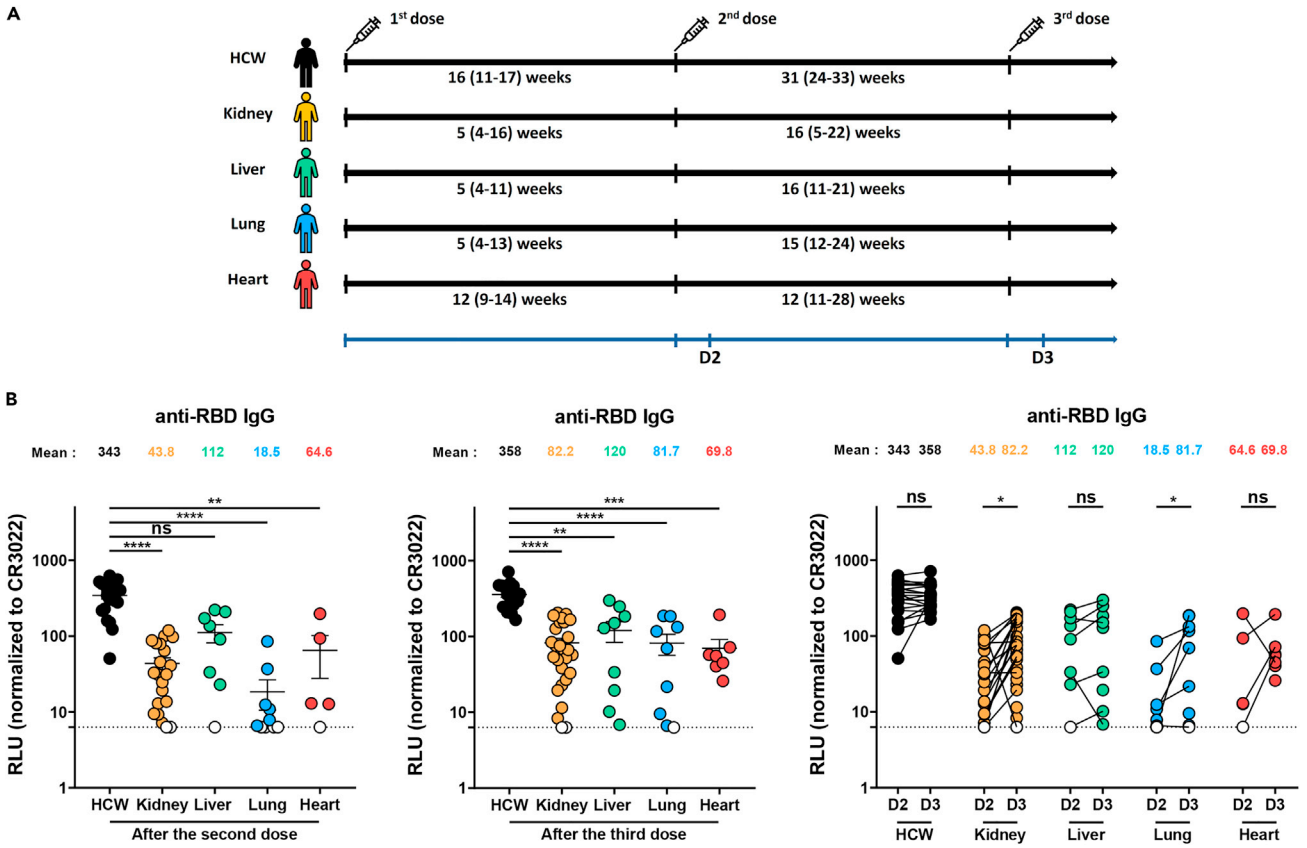

Figure 1. Elicitation of RBD-specific antibodies in SOTR and HCW after mRNA vaccination

(A) SARS-CoV-2 vaccine cohorts' design.

(B) Indirect ELISA was performed by incubating plasma samples from SOTR or HCW with recombinant SARS-CoV-2 RBD protein. Anti-RBD Ab binding was detected using HRP-conjugated anti-human IgG. Relative light unit (RLU) values obtained with BSA (negative control) were subtracted and further normalized to the signal obtained with the anti-RBD CR3022 mAb presents in each plate. **Left panel** shows the values obtained after the second dose, and **middle panel** after the third dose. **Right panel** shows the difference obtained between D2 (post second dose) and D3 (post third dose) for every group. Symbols represent biologically independent samples from SOTR and HCW. Lines connect data from the same donor. Undetectable measures are represented as white symbols, and limits of detection are plotted. Error bars indicate means ± SEM. (*$p < 0.05$; **$p < 0.01$; ***$p < 0.001$; ****$p < 0.0001$; ns, non-significant). HCW, n = 20 at D2 and D3, for kidney recipients, n = 21 at D2 and n = 27 at D3, for liver recipients, n = 9 at D2 and n = 8 at D3, for lung recipients, n = 9 at D2 and D3, and for heart recipients, n = 5 at D2 and n = 7 at D3.

We also evaluated the recognition of the human HKU1 *Betacoronavirus* S glycoprotein (Figure 2D). HKU1 is an endemic coronavirus that causes common colds and is highly prevalent in the population (Chan et al., 2009; Rees et al., 2021). No significant differences between HCW and SOTR were observed after the second and the third doses of the vaccine, indicating that transplantation and associated immunosuppression regimens did not affect the level of circulating Abs elicited before vaccination.

Functional activities of vaccine-elicited antibodies

We evaluated functional activities of vaccine-elicited Abs after the second and third doses of mRNA vaccine (Figure 3). We measured Fc-mediated effector functions using a well-described antibody-dependent cellular cytotoxicity (ADCC) assay (Anand et al., 2021; Beaudoin-Bussières et al., 2020,2021; Ullah et al., 2021). Plasma from HCW presented robust ADCC activity after the second dose that was restored to the same level by the third dose (Figure 3A). The second dose elicited ADCC-mediating Abs in liver and heart recipients that reached similar levels of activity as in HCW. This is in contrast with significant lower ADCC activity elicited after the second dose in kidney and lung recipients. The boost led to a significant increase in ADCC activity in these recipients. Importantly, the third dose elicited ADCC activity in all SOTR similar to the one observed in HCW.

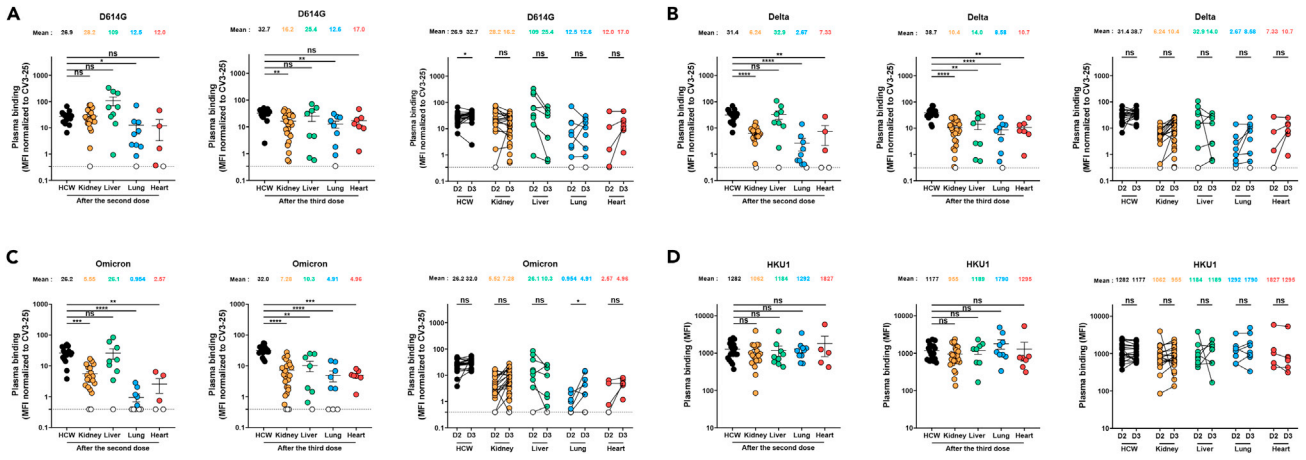

Figure 2. Binding of vaccine-elicited antibodies to SARS-CoV-2 Spike variants and the human HKU1 *Betacoronavirus* in SOTR and HCW after mRNA vaccination

293T cells were transfected with the indicated full-length S from different SARS-CoV-2 variants and HCoV-HKU1 and stained with the CV3-25 Ab or with plasma from SOTR or HCW. The values represent the median fluorescence intensities (MFI) normalized by CV3-25 Ab binding (A–C) or the MFI (D). **Left panel** shows the values obtained after the second dose, and **middle panel** after the third dose. **Right panel** shows the differences obtained between D2 (post second dose) and D3 (post third dose) for every group. Symbols represent biologically independent samples from SOTR and HCW. Lines connect data from the same donor. Undetectable measures are represented as white symbols, and limits of detection are plotted. Error bars indicate means ± SEM. (*$p < 0.05$; **$p < 0.01$; ***$p < 0.001$; ****$p < 0.0001$; ns, non-significant). HCW, n = 20 at D2 and D3, for kidney recipients, n = 21 at D2 and n = 27 at D3, for liver recipients, n = 9 at D2 and n = 8 at D3, for lung recipients, n = 9 at D2 and D3, and for heart recipients, n = 5 at D2 and n = 7 at D3.

We also measured the neutralizing activity of the vaccine-induced Abs, against pseudoviruses carrying SARS-CoV-2 S (Figures 3B–3D). When assessing the neutralizing activity against the D614G S, we observed that the second dose elicited Abs with neutralizing activity in liver recipients (Figure 3B). In other SOTR, very low levels of neutralizing Abs were detected, especially in lung recipients. As observed for ADCC activity, the boost increased the neutralization activity in kidney and lung recipients. However, even after the third dose, SOTR did not reach the same levels of neutralizing Abs as in HCW, with the exception of liver recipients.

We also measured the neutralizing activity against pseudoviruses carrying the Delta and Omicron Spikes (Figures 3C and 3D). In HCW, the second dose of mRNA vaccine administered with a 16-weeks interval, led to high levels of Abs able to neutralize these variants, as previously described (Chatterjee et al., 2022; Payne et al., 2021; Tauzin et al., 2022a). In contrast, SOTR elicited very low levels of neutralizing Abs against Delta and Omicron variants after the second dose and, although the boost led to a slight increase of the neutralization activity, this remained lower than in HCW.

When comparing the neutralizing activity between the SARS-CoV-2 variants (Figure S3), Delta was less efficiently neutralized in HCW than D614G at the two different time points (Figure S3A). For kidney and liver recipients, Omicron and Delta VOCs were less neutralized than D614G (Figures S3B–S3C). For other SOTR, neutralization activity was too weak to measure significant differences (Figures S3D–S3E).

Anti-RBD avidity of vaccine-elicited antibodies

We also used a surrogate assay for antibody maturation by measuring the avidity for the RBD of vaccine-elicited Abs, using a previously described assay (Björkman et al., 1999; Fialová et al., 2017; Tauzin et al., 2022a,2022b,2022c). Briefly, plasma samples were tested in parallel by ELISA with washing steps having or not having a chaotropic agent (8M urea), measuring respectively the level of IgG with high avidity for the RBD and the level of total anti-RBD IgG. The RBD-avidity index corresponds to the proportion of high avidity IgG among the total anti-RBD IgG (Figure 4), and provides an overall idea of antibody maturation (Björkman et al., 1999; Fialová et al., 2017; Tauzin et al., 2022a,2022b,2022c).

In HCW, the second dose of the mRNA vaccine elicited IgG with high avidity, that was not further improved by the boost (Figure 4), as recently described (Tauzin et al., 2022a). In contrast, in SOTR who developed Abs able to recognize the RBD, the avidity was significantly lower than in HCW (Figures 1B and 4). The third dose

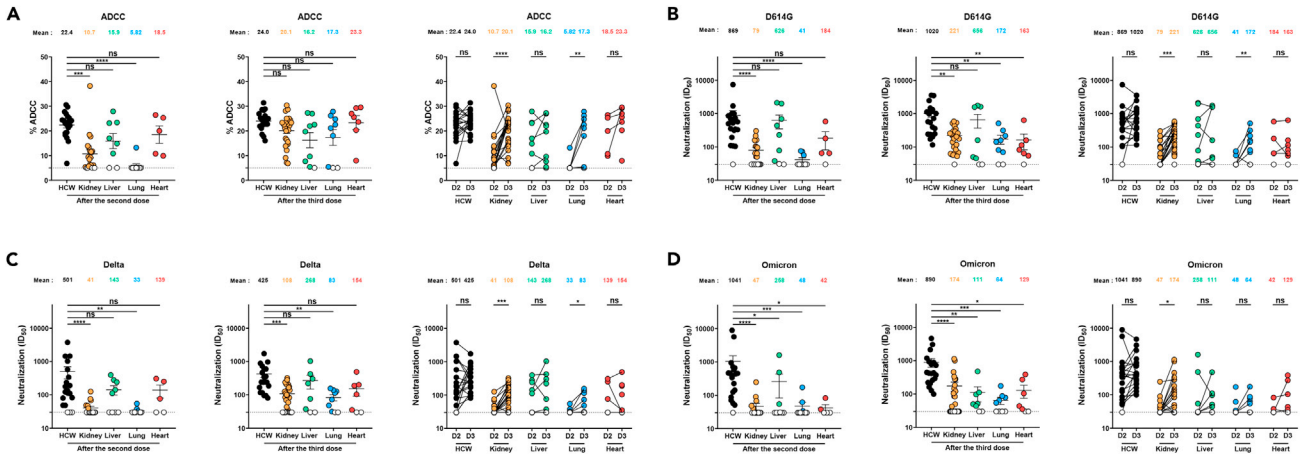

Figure 3. Fc-mediated effector functions and neutralization activities in SOTR and HCW after mRNA vaccination

(A) CEM.NKr parental cells were mixed at a 1:1 ratio with CEM.NKr-Spike cells and were used as target cells. PBMCs from uninfected donors were used as effector cells in a FACS-based ADCC assay.

(B–D) Neutralizing activity was measured by incubating pseudoviruses bearing SARS-CoV-2 S glycoproteins ((B) D614G, (C) Delta and (D) Omicron), with serial dilutions of plasma for 1hat 37°C before infecting 293T-ACE2 cells. Neutralization half maximal inhibitory serum dilution (ID_{50}) values were determined using a normalized non-linear regression using GraphPad Prism software. **Left panel** shows the values obtained after the second dose, and **middle panel** after the third dose. **Right panel** shows the differences obtained between D2 (post second dose) and D3 (post third dose) for every group. Symbols represent biologically independent samples from SOTR and HCW. Lines connect data from the same donor. Undetectable measures are represented as white symbols, and limits of detection are plotted. Error bars indicate means ± SEM. (*$p < 0.05$; **$p < 0.01$; ***$p < 0.001$; ****$p < 0.0001$; ns, non-significant). HCW, n = 20 at D2 and D3, for kidney recipients, n = 21 at D2 and n = 27 at D3, for liver recipients, n = 9 at D2 and n = 8 at D3, for lung recipients, n = 9 at D2 and D3, and for heart recipients, n = 5 at D2 and n = 7 at D3.

of mRNA vaccine increased RBD avidity in SOTR but, with the exception of liver recipients, remained significantly lower than in HCW.

Impact of immunosuppressive treatment doses on the level of SARS-CoV-2 IgG elicited by vaccination

Immunosuppressants belong to different classes of inhibitors and can prevent cell activation, cytokine production, differentiation, and/or proliferation, depending on the mechanisms of action of the drug (Roberts and Fishman, 2021; Suthanthiran et al., 1996). We evaluated whether the daily dose of immunosuppressant administered to the SOTR had an impact on the level of anti-RBD IgG induced after vaccination (Figure 5).

After the second dose of vaccine (D2), SOTR who received high daily dosing of prednisone and mycophenolate mofetil/mycophenolate sodium had lower levels of IgG than SOTR treated at lower daily dosing. Of interest, no significant differences were observed after the third dose, suggesting that, even under strong immunosuppressive treatment, SOTR can initiate humoral responses by repeated antigen exposure. Tacrolimus concentrations did not affect the level of vaccine elicited IgG, indicating that humoral responses are differently affected depending on the class and concentration of the immunosuppressive treatment (Figure 5). However, given the wide person-to-person variability in tacrolimus metabolism, it is also possible that tacrolimus daily dose does not reflect its exposure as much as other immunosuppressive agents studied. The low numbers of SOTR receiving azathioprine, sirolimus, and cyclosporine precluded as from evaluating their impact in vaccine-elicited responses.

Integrated analysis of vaccine responses elicited in solid organ transplant recipients

We evaluated the network of pair-wise correlations among all studied immune variables on the HCW and the different SOTR groups (Figure 6). For HCW, we observed that after the second dose all immune variables tested were involved in a dense network of positive correlations. After the boost, we did not observe major differences in the network of correlations, suggesting that the third dose did not induce qualitatively different humoral responses in HCW. For lung and heart recipients, who received strong immunosuppressive regimens that affected anti-RBD IgG level (Table 1, Figures 5 and S1), we observed that all immune variables were weakly interconnected after the second dose and the third dose did not strongly increase the network. Immune variables were slightly more interconnected for kidney recipients, which aligns

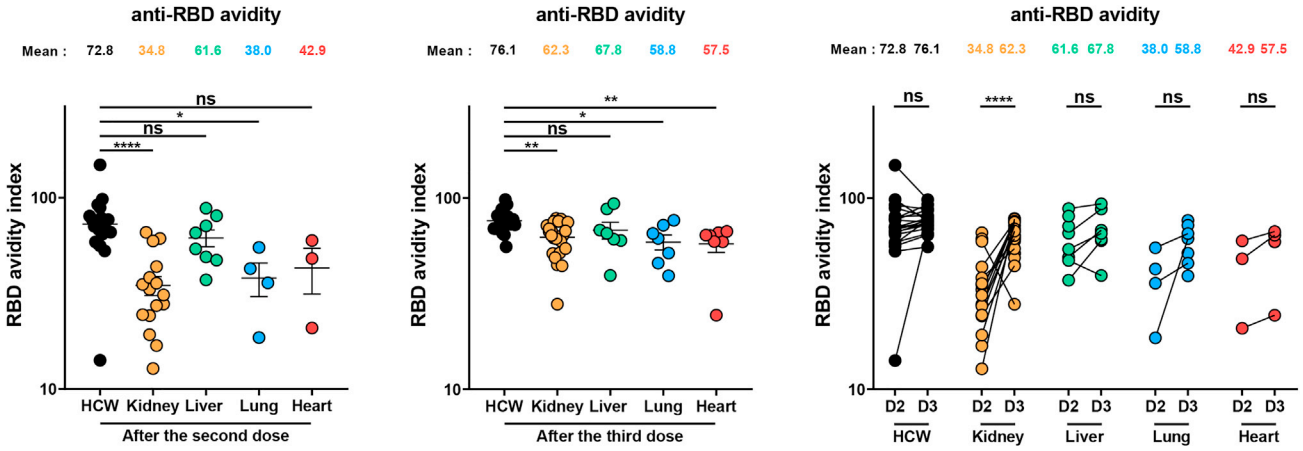

Figure 4. Anti-RBD avidity of vaccine-elicited antibodies in SOTR and HCW after mRNA vaccination

Indirect ELISA and stringent ELISA were performed by incubating plasma samples from SOTR and HCW with recombinant SARS-CoV-2 RBD protein. Anti-RBD Ab binding was detected using HRP-conjugated anti-human IgG. The RBD avidity index corresponded to the RLU value obtained for every plasma sample with the stringent (8M urea) ELISA divided by that obtained with the 0M urea ELISA. **Left panel** shows the values obtained after the second dose, and **middle panel** after the third dose. **Right panel** shows the differences obtained between D2 (post second dose) and D3 (post third dose) for every group. Symbols represent biologically independent samples from SOTR and HCW. Lines connect data from the same donor. Error bars indicate means ± SEM. (*p < 0.05; **p < 0.01; ****p < 0.0001; ns, non-significant). For HCW, n = 20 at D2 and D3, for kidney recipients, n = 17 at D2 and n = 24 at D3, for liver recipients, n = 8 at D2 and n = 7 at D3, for lung recipients, n = 4 at D2 and n = 7 at D3, and for heart recipients, n = 3 at D2 and n = 7 at D3.

with their lower immunosuppressive regimen compared to heart and lung recipients (Figure S1). For liver recipients, the network of correlation was less dense than in HCW after the second dose as observed for the other groups of SOTR. Of interest, this group of SOTR mainly treated with tacrolimus, that did not impact the level of IgG, and low dose of prednisone and mycophenolate mofetil/mycophenolate sodium (Figure S1), the third dose of the mRNA vaccine induced a dense network of correlations, which was in a comparable range as in HCW.

DISCUSSION

Although a large part of the world population is vaccinated with two or three doses of SARS-CoV-2 vaccines, some population groups remain vulnerable to SARS-CoV-2 infection and most importantly to severe outcomes. Here we demonstrate that SOTR, known to respond less efficiently to vaccination because of their chronic immunosuppressive regimen (Kumar et al., 2011; Stucchi et al., 2018), elicited poor humoral responses after the second dose of SARS-CoV-2 mRNA vaccine, compared to HCW. The boost induced an increase of these responses, but they did not reach the same level as observed in HCW.

An important concern about the evolving pandemic is the frequent apparition of variants. It was previously shown that the 3–4 weeks standard interval of vaccination leads to weak neutralizing Abs against several VOCs in the general population (Chatterjee et al., 2022; Payne et al., 2021; Tauzin et al., 2022a,2022c). However, administering a boost strongly enhances the breadth of neutralization activity against these variants (Nemet et al., 2022; Schmidt et al., 2022; Tauzin et al., 2022a). In SOTR, we did not observe a significant increase in the breadth of recognition and neutralization of these variants, suggesting an inability in Abs maturation in most of these individuals. This is supported by the poor anti-RBD avidity detected in these individuals, likely reflecting poor B cells maturation compared to HCW.

Of interest, we observed that SOTR elicited Abs with ADCC activity comparable to HCW after the third dose of the mRNA vaccine. There is increasing evidence showing that Fc-mediated effector functions play an important role in the protection against severe outcomes of SARS-CoV-2 (Anand et al., 2021; Richardson et al., 2022; Tauzin et al., 2021). However, whether this will suffice to protect SOTR from severe outcomes caused by SARS-CoV-2 remains unknown.

We also noted some differences in humoral responses, depending on the transplanted organ. Notably, we observed that liver recipients had better humoral responses than other SOTR groups. Previous studies have

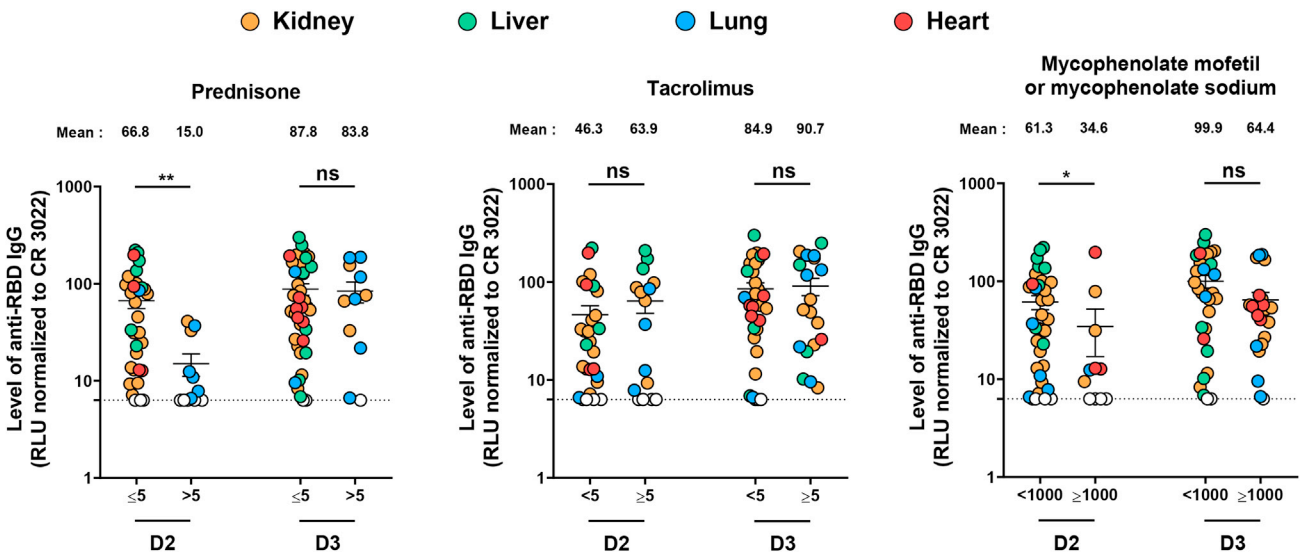

Figure 5. Effect of immunosuppressive drug on the level of anti-RBD IgG elicited by SARS-CoV-2 vaccination in SOTR

The graphs show the level of anti-RBD IgG measured after the second (D2) and the third (D3) dose of vaccine in kidney (yellow), liver (green), lung (blue) and heart (red) recipients, depending of the daily dose administered (≤5 vs > 5 mg/day for prednisone; <5 vs ≥ 5 mg/day for tacrolimus; <1000 vs ≥ 1000 mg/day for mycophenolate mofetil or mycophenolate sodium). Symbols represent biologically independent samples from transplant recipients. Undetectable measures are represented as white symbols, and limits of detection are plotted. Error bars indicate means ± SEM. (*$p < 0.05$; **$p < 0.01$; ns, non-significant). For kidney recipients, n = 21 at D2 and n = 27 at D3, for liver recipients, n = 9 at D2 and n = 8 at D3, for lung recipients, n = 9 at D2 and D3, and for heart recipients, n = 5 at D2 and n = 7 at D3.

shown that some class of immunosuppressants, depending on their concentration, had an impact on humoral and cellular responses after SARS-CoV-2 mRNA vaccination (Charmetant et al., 2022; Netti et al., 2022). We observed that SOTR treated with high dose of prednisone and mycophenolate mofetil/mycophenolate sodium had lower Abs responses, whereas no significant differences were observed with tacrolimus. In our SOTR cohort, liver recipients were mostly treated with tacrolimus and/or low doses of prednisone and mycophenolate mofetil/mycophenolate sodium, which probably explains why they had better humoral responses. However, a previous study reported poor humoral responses in liver recipients (Rabinowich et al., 2021). This is likely due to the differences in immunosuppressive regimens used on these different cohorts. Further work is needed to understand the correlation between specific immunosuppressive regimens and vaccination outcome, taking into account the dose and type of immunosuppressive agents, and response to SARS-CoV-2 vaccines. This also highlights the importance of evaluating the different SOTR groups independently regarding the decisions on the follow-up of vaccinations that needs to be adapted to each SOTR group.

Limitations of the study

A limitation of this study is the low number of SOTR studied which could affect the power of the correlation between humoral responses. Another limitation is the interval between the doses which was not the same depending on the group. For HCW, it was extended to 16 weeks between the two first doses, a vaccine regimen that proved to be better than a 3–4 weeks regimen in healthy individuals (Payne et al., 2021; Tauzin et al., 2022c). However, the interval was 5 weeks for SOTR, in agreement with Canadian guidelines for immunocompromised individuals (CIG, 2021). Another limitation of the study is the age of heart recipients which were older than in the other SOTR groups studied here.

STAR★METHODS

Detailed methods are provided in the online version of this paper and include the following:

- KEY RESOURCES TABLE
- RESOURCE AVAILABILITY
  - Lead contact
  - Materials availability
  - Data and code availability

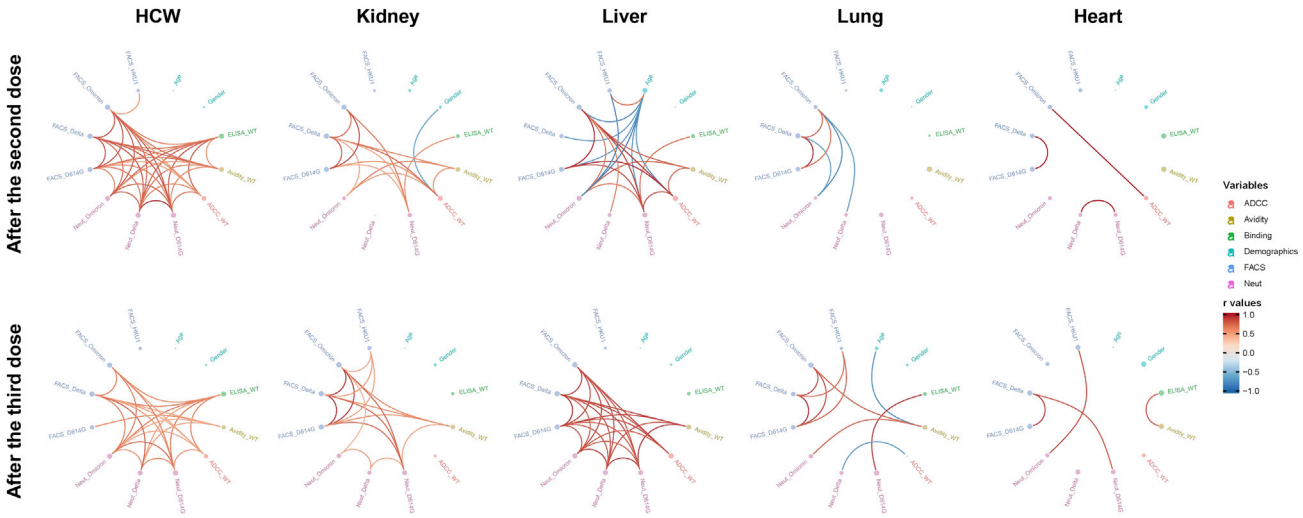

Figure 6. Mesh correlations of humoral response variables in SOTR and HCW after mRNA vaccination

Edge bundling correlation plots where red and blue edges represent positive and negative correlations between connected variables, respectively. Only significant correlations ($p < 0.05$, Spearman rank test) are displayed. Nodes are color coded based on the grouping of variables according to the legend. Node size corresponds to the degree of relatedness of correlations. Edge bundling plots are shown for correlation analyses using ten different datasets, i.e., HCW and kidney, liver, lung or heart transplant recipients after the second and third doses of mRNA vaccination. HCW, n = 20 at D2 and D3, for kidney recipients, n = 21 at D2 and n = 27 at D3, for liver recipients, n = 9 at D2 and n = 8 at D3, for lung recipients, n = 9 at D2 and D3, and for heart recipients, n = 5 at D2 and n = 7 at D3.

SUPPLEMENTAL INFORMATION

Supplemental information can be found online at https://doi.org/10.1016/j.isci.2022.104990.

ACKNOWLEDGMENTS

The authors are grateful to the donors and recipients who participated in this study. The authors thank the CRCHUM BSL3 and Flow Cytometry Platforms for technical assistance. We thank Dr. M. Gordon Joyce (US MHRP) for the monoclonal antibody CR3022. We also thank Demitra Yotis, Amani Mahroug, Yizou Zhao, Annie Karakeussian Rimbaud, Éric Ducas and Isabelle Paré for their contribution on the transplant cohort. The graphical abstract was created using BioRender.com. This work was supported by le Ministère de l'Économie et de l'Innovation du Québec, Programme de soutien aux organismes de recherche et d'innovation to A.F. and by the Fondation du CHUM. This work was also supported by a CIHR foundation grant #352417, by a CIHR operating Pandemic and Health Emergencies Research grant #177958, to A.F., and by an Exceptional Fund COVID-19 from the Canada Foundation for Innovation (CFI) #41027 to D.E.K. and A.F. This work was also supported by a FRQS Pandemic Initiatives COVID-19 grant #308941 to M.J.H and in-kind contribution from Canadian Donation and Transplantation Research Program (CDTRP). Work on variants presented was also supported by the

Sentinelle COVID Quebec network led by the LSPQ in collaboration with Fonds de Recherche du Québec - Santé (FRQS) to A.F. A.F. is the recipient of Canada Research Chair on Retroviral Entry no. RCHS0235 950–232424. M.-J. H. and H.C. holds the Shire Chair in Nephrology, Transplantation and Renal Regeneration of Université de Montréal. C.T holds the Pfizer/Université deMontréal Chair on HIV translational research. V.M.L. is supported by a FRQS Junior 1 salary award. D.E.K. is a FRQS Merit Research Scholar. H.C. is supported by a Junior 2 Fonds de Recherche du Québec - Santé Award. G.B.B. is the recipient of a FRQS PhD fellowship. The funders had no role in study design, data collection and analysis, decision to publish, or preparation of the manuscript. We declare no competing interests.

AUTHOR CONTRIBUTIONS

A.T., M.D., M.J.H., and A.F. conceived the study. A.T., G.B.B., S.Y.G., D.C., C.B., P.L., G.G.L. M.D., M.J.H., and A.F. performed, analyzed, and interpreted the experiments. A.T. and R.D. performed statistical analysis. G.B.B., S.Y.G., G.G.L., G.G., J.T., M.D., M.J.H., and A.F. contributed unique reagents. N.R., Z.K. C.T., D.E.K., M.J.H., H.C., and V.M.-L. collected and provided clinical samples. D.E.K., H.C, M.C., R.B., M.D., M.J.H., and A.F provided scientific input. A.T. and A.F. wrote the manuscript with inputs from others. Every author has read, edited, and approved the final manuscript.

DECLARATION OF INTERESTS

The authors declare no competing interests.

Received: May 20, 2022
Revised: July 4, 2022
Accepted: August 17, 2022
Published: September 16, 2022

REFERENCES

Anand, S.P., Prévost, J., Nayrac, M., Beaudoin-Bussières, G., Benlarbi, M., Gasser, R., Brassard, N., Laumaea, A., Gong, S.Y., Bourassa, C., et al. (2021). Longitudinal analysis of humoral immunity against SARS-CoV-2 Spike in convalescent individuals up to eight months post-symptom onset. Cell Rep. Med. *2*. https://doi.org/10.1016/j.xcrm.2021.100290.

Anand, S.P., Prévost, J., Richard, J., Perreault, J., Tremblay, T., Drouin, M., Fournier, M.-J., Lewin, A., Bazin, R., and Finzi, A. (2020). High-throughput Detection of Antibodies Targeting the SARS-CoV-2 Spike in Longitudinal Convalescent Plasma Samples (Microbiology).

Ariën, K.K., Heyndrickx, L., Michiels, J., Vereecken, K., Van Lent, K., Coppens, S., Willems, B., Pannus, P., Martens, G.A., Van Esbroeck, M., et al. (2022). Three doses of BNT162b2 vaccine confer neutralising antibody capacity against the SARS-CoV-2 Omicron variant. NPJ Vaccines *7*, 35. https://doi.org/10.1038/s41541-022-00459-z.

AST (2022). Joint Statement about COVID-19 Vaccination in Organ Transplant Candidates and Recipients. https://www.myast.org/sites/default/files/03-13-22%20ISHLT-AST-ASTS%20joint%20society%20guidance%20vaccine_v9.pdf.

Baden, L.R., El Sahly, H.M., Essink, B., Kotloff, K., Frey, S., Novak, R., Diemert, D., Spector, S.A., Rouphael, N., Creech, C.B., et al. (2021). Efficacy and safety of the mRNA-1273 SARS-CoV-2 vaccine. N. Engl. J. Med. *384*, 403–416. https://doi.org/10.1056/NEJMoa2035389.

Beaudoin-Bussières, G., Laumaea, A., Anand, S.P., Prévost, J., Gasser, R., Goyette, G., Medjahed, H., Perreault, J., Tremblay, T., Lewin, A., et al. (2020). Decline of humoral responses against SARS-CoV-2 spike in convalescent individuals. mBio *11*, e02590-20. https://doi.org/10.1128/mBio.02590-20.

Beaudoin-Bussières, G., Richard, J., Prévost, J., Goyette, G., and Finzi, A. (2021). A new flow cytometry assay to measure antibody-dependent cellular cytotoxicity against SARS-CoV-2 Spike-expressing cells. STAR Protoc. *2*, 100851. https://doi.org/10.1016/j.xpro.2021.100851.

Björkman, C., Näslund, K., Stenlund, S., Maley, S.W., Buxton, D., and Uggla, A. (1999). An IgG avidity ELISA to discriminate between recent and chronic neospora caninum infection. J. Vet. Diagn. Invest. *11*, 41–44. https://doi.org/10.1177/104063879901100106.

Caillard, S., Chavarot, N., Bertrand, D., Kamar, N., Thaunat, O., Moal, V., Masset, C., Hazzan, M., Gatault, P., Sicard, A., et al. (2021). Occurrence of severe COVID-19 in vaccinated transplant patients. Kidney Int. *100*, 477–479. https://doi.org/10.1016/j.kint.2021.05.011.

Chan, C.M., Tse, H., Wong, S.S.Y., Woo, P.C.Y., Lau, S.K.P., Chen, L., Zheng, B.J., Huang, J.D., and Yuen, K.Y. (2009). Examination of seroprevalence of coronavirus HKU1 infection with S protein-based ELISA and neutralization assay against viral spike pseudotyped virus. J. Clin. Virol. *45*, 54–60. https://doi.org/10.1016/j.jcv.2009.02.011.

Charmetant, X., Espi, M., Benotmane, I., Barateau, V., Heibel, F., Buron, F., Gautier-Vargas, G., Delafosse, M., Perrin, P., Koenig, A., et al. (2022). Infection or a third dose of mRNA vaccine elicits neutralizing antibody responses against SARS-CoV-2 in kidney transplant recipients. Sci. Transl. Med. *14*, eabl6141. https://doi.org/10.1126/scitranslmed.abl6141.

Chatterjee, D., Tauzin, A., Marchitto, L., Gong, S.Y., Boutin, M., Bourassa, C., Beaudoin-Bussières, G., Bo, Y., Ding, S., Laumaea, A., et al. (2022). SARS-CoV-2 Omicron Spike recognition by plasma from individuals receiving BNT162b2 mRNA vaccination with a 16-week interval between doses. Cell Rep. *38*. https://doi.org/10.1016/j.celrep.2022.110429.

CST (2022). National Transplant Consensus Guidance on COVID-19 Vaccine. chrome-https://www.cst-transplant.ca/_Library/Coronavirus/National_Transplant_Consensus_Guidance_on_COVID_Vaccine_2022_1_final_1_.pdf.

Danziger-Isakov, L., Blumberg, E.A., Manuel, O., and Sester, M. (2021). Impact of COVID-19 in solid organ transplant recipients. Am. J. Transplant. *21*, 925–937. https://doi.org/10.1111/ajt.16449.

Fialová, L., Petráčková, M., and Kuchař, O. (2017). Comparison of different enzyme-linked immunosorbent assay methods for avidity determination of antiphospholipid antibodies. J. Clin. Lab. Anal. *31*, e22121. https://doi.org/10.1002/jcla.22121.

Gong, S.Y., Chatterjee, D., Richard, J., Prévost, J., Tauzin, A., Gasser, R., Bo, Y., Vézina, D., Goyette, G., Gendron-Lepage, G., et al. (2021). Contribution of single mutations to selected SARS-CoV-2 emerging variants spike antigenicity. Virology *563*, 134–145. https://doi.org/10.1016/j.virol.2021.09.001.

Jennewein, M.F., MacCamy, A.J., Akins, N.R., Feng, J., Homad, L.J., Hurlburt, N.K., Seydoux, E., Wan, Y.-H., Stuart, A.B., Edara, V.V., et al. (2021).

Isolation and characterization of cross-neutralizing coronavirus antibodies from COVID-19+ subjects. Cell Rep. *36*, 109353. https://doi.org/10.1016/j.celrep.2021.109353.

Kumar, D., Blumberg, E.A., Danziger-Isakov, L., Kotton, C.N., Halasa, N.B., Ison, M.G., Avery, R.K., Green, M., Allen, U.D., Edwards, K.M., et al. (2011). Influenza vaccination in the organ transplant recipient: review and summary recommendations. Am. J. Transplant. *11*, 2020–2030. https://doi.org/10.1111/j.1600-6143.2011.03753.x.

Kumar, S., Thambiraja, T.S., Karuppanan, K., and Subramaniam, G. (2022). Omicron and Delta variant of SARS-CoV-2: a comparative computational study of spike protein. J. Med. Virol. *94*, 1641–1649. https://doi.org/10.1002/jmv.27526.

Lauring, A.S., Tenforde, M.W., Chappell, J.D., Gaglani, M., Ginde, A.A., McNeal, T., Ghamande, S., Douin, D.J., Talbot, H.K., Casey, J.D., et al. (2022). Clinical severity of, and effectiveness of mRNA vaccines against, covid-19 from omicron, delta, and alpha SARS-CoV-2 variants in the United States: prospective observational study. BMJ *376*, e069761. https://doi.org/10.1136/bmj-2021-069761.

Li, W., Chen, Y., Prévost, J., Ullah, I., Lu, M., Gong, S.Y., Tauzin, A., Gasser, R., Vézina, D., Anand, S.P., et al. (2022). Structural basis and mode of action for two broadly neutralizing antibodies against SARS-CoV-2 emerging variants of concern. Cell Rep. *38*, 110210. https://doi.org/10.1016/j.celrep.2021.110210.

Miele, M., Busà, R., Russelli, G., Sorrentino, M.C., Di Bella, M., Timoneri, F., Mularoni, A., Panarello, G., Vitulo, P., Conaldi, P.G., and Bulati, M. (2021). Impaired anti-SARS-CoV-2 humoral and cellular immune response induced by pfizer-BioNTech BNT162b2 mRNA vaccine in solid organ transplanted patients. Am. J. Transplant. *21*, 2919–2921. https://doi.org/10.1111/ajt.16702.

Nayrac, M., Dubé, M., Sannier, G., Nicolas, A., Marchitto, L., Tastet, O., Tauzin, A., Brassard, N., Lima-Barbosa, R., Beaudoin-Bussières, G., et al. (2022). Temporal associations of B and T cell immunity with robust vaccine responsiveness in a 16-week interval BNT162b2 regimen. Cell Rep. *39*, 111013. https://doi.org/10.1016/j.celrep.2022.111013.

Nemet, I., Kliker, L., Lustig, Y., Zuckerman, N., Erster, O., Cohen, C., Kreiss, Y., Alroy-Preis, S., Regev-Yochay, G., Mendelson, E., and Mandelboim, M. (2022). Third BNT162b2 vaccination neutralization of SARS-CoV-2 omicron infection. N. Engl. J. Med. *386*, 492–494. https://doi.org/10.1056/NEJMc2119358.

Netti, G.S., Infante, B., Troise, D., Mercuri, S., Panico, M., Spadaccino, F., Catalano, V., Gigante, M., Simone, S., Pontrelli, P., et al. (2022). mTOR inhibitors improve both humoral and cellular response to SARS-CoV-2 messenger RNA BNT16b2 vaccine in kidney transplant recipients. Am. J. Transplant. *22*, 1475–1482. https://doi.org/10.1111/ajt.16958.

Payne, R.P., Longet, S., Austin, J.A., Skelly, D.T., Dejnirattisai, W., Adele, S., Meardon, N., Faustini, S., Al-Taei, S., Moore, S.C., et al. (2021). Immunogenicity of standard and extended dosing intervals of BNT162b2 mRNA vaccine. Cell *184*, 5699–5714.e11. https://doi.org/10.1016/j.cell.2021.10.011.

Pereira, M.R., Mohan, S., Cohen, D.J., Husain, S.A., Dube, G.K., Ratner, L.E., Arcasoy, S., Aversa, M.M., Benvenuto, L.J., Dadhania, D.M., et al. (2020). COVID-19 in solid organ transplant recipients: initial report from the US epicenter. Am. J. Transplant. *20*, 1800–1808. https://doi.org/10.1111/ajt.15941.

P.H.A. of CIG (2021). COVID-19 Vaccine: Canadian Immunization Guide. https://www.canada.ca/en/public-health/services/publications/healthy-living/canadian-immunization-guide-part-4-active-vaccines/page-26-covid-19-vaccine.html.

Planas, D., Saunders, N., Maes, P., Guivel-Benhassine, F., Planchais, C., Buchrieser, J., Bolland, W.-H., Porrot, F., Staropoli, I., Lemoine, F., et al. (2021). Considerable escape of SARS-CoV-2 Omicron to antibody neutralization. Nature *602*, 671–675. https://doi.org/10.1038/s41586-021-04389-z.

Polack, F.P., Thomas, S.J., Kitchin, N., Absalon, J., Gurtman, A., Lockhart, S., Perez, J.L., Pérez Marc, G., Moreira, E.D., Zerbini, C., et al. (2020). Safety and efficacy of the BNT162b2 mRNA covid-19 vaccine. N. Engl. J. Med. *383*, 2603–2615. https://doi.org/10.1056/NEJMoa2034577.

Prévost, J., Gasser, R., Beaudoin-Bussières, G., Richard, J., Duerr, R., Laumaea, A., Anand, S.P., Goyette, G., Benlarbi, M., Ding, S., et al. (2020). Cross-sectional evaluation of humoral responses against SARS-CoV-2 spike. Cell Rep. Med. *1*, 100126. https://doi.org/10.1016/j.xcrm.2020.100126.

R Core Team (2014). R: A Language and Environment for Statistical Computing (R Foundation for Statistical Computing). http://www.R-project.org/.

Rabinowich, L., Grupper, A., Baruch, R., Ben-Yehoyada, M., Halperin, T., Turner, D., Katchman, E., Levi, S., Houri, I., Lubezky, N., et al. (2021). Low immunogenicity to SARS-CoV-2 vaccination among liver transplant recipients. J. Hepatol. *75*, 435–438. https://doi.org/10.1016/j.jhep.2021.04.020.

Rees, E.M., Waterlow, N.R.; Centre for the Mathematical Modelling of Infectious Diseases COVID-19 Working Group, and Kucharski, A.J. (2021). Estimating the duration of seropositivity of human seasonal coronaviruses using seroprevalence studies. Wellcome Open Res. *6*, 138. https://doi.org/10.12688/wellcomeopenres.16701.3.

Richardson, S.I., Manamela, N.P., Motsoeneng, B.M., Kaldine, H., Ayres, F., Makhado, Z., Mennen, M., Skelem, S., Williams, N., Sullivan, N.J., et al. (2022). SARS-CoV-2 Beta and Delta variants trigger Fc effector function with increased cross-reactivity. Cell Rep. Med. *3*, 100510. https://doi.org/10.1016/j.xcrm.2022.100510.

Rincon-Arevalo, H., Choi, M., Stefanski, A.-L., Halleck, F., Weber, U., Szelinski, F., Jahrsdörfer, B., Schrezenmeier, H., Ludwig, C., Sattler, A., et al. (2021). Impaired humoral immunity to SARS-CoV-2 BNT162b2 vaccine in kidney transplant recipients and dialysis patients. Sci. Immunol. *6*, eabj1031. https://doi.org/10.1126/sciimmunol.abj1031.

Roberts, M.B., and Fishman, J.A. (2021). Immunosuppressive agents and infectious risk in transplantation: managing the "net state of immunosuppression". Clin. Infect. Dis. *73*, e1302–e1317. https://doi.org/10.1093/cid/ciaa1189.

Schmidt, F., Muecksch, F., Weisblum, Y., Da Silva, J., Bednarski, E., Cho, A., Wang, Z., Gaebler, C., Caskey, M., Nussenzweig, M.C., et al. (2022). Plasma neutralization of the SARS-CoV-2 omicron variant. N. Engl. J. Med. *386*, 599–601. https://doi.org/10.1056/NEJMc2119641.

Sheikhi, K., Shirzadfar, H., and Sheikhi, M. (2020). A review on novel coronavirus (Covid-19): symptoms, transmission and diagnosis tests. Res. Infect. Dis. Trop. Med. *2*, 1–8. https://doi.org/10.33702/ridtm.2020.2.1.1.

Stucchi, R.S.B., Lopes, M.H., Kumar, D., and Manuel, O. (2018). Vaccine recommendations for solid-organ transplant recipients and donors. Transplantation *102*, S72–S80. https://doi.org/10.1097/TP.0000000000002012.

Stumpf, J., Siepmann, T., Lindner, T., Karger, C., Schwöbel, J., Anders, L., Faulhaber-Walter, R., Schewe, J., Martin, H., Schirutschke, H., et al. (2021). Humoral and cellular immunity to SARS-CoV-2 vaccination in renal transplant versus dialysis patients: a prospective, multicenter observational study using mRNA-1273 or BNT162b2 mRNA vaccine. Lancet Reg. Health. Eur. *9*, 100178. https://doi.org/10.1016/j.lanepe.2021.100178.

Suthanthiran, M., Morris, R.E., and Strom, T.B. (1996). Immunosuppressants: cellular and molecular mechanisms of action. Am. J. Kidney Dis. *28*, 159–172. https://doi.org/10.1016/s0272-6386(96)90297-8.

Tauzin, A., Gendron-Lepage, G., Nayrac, M., Anand, S.P., Bourassa, C., Medjahed, H., Goyette, G., Dubé, M., Bazin, R., Kaufmann, D.E., and Finzi, A. (2022b). Evolution of anti-RBD IgG avidity following SARS-CoV-2 infection. Viruses *14*, 532. https://doi.org/10.3390/v14030532.

Tauzin, A., Gong, S.Y., Beaudoin-Bussières, G., Vézina, D., Gasser, R., Nault, L., Marchitto, L., Benlarbi, M., Chatterjee, D., Nayrac, M., et al. (2022c). Strong humoral immune responses against SARS-CoV-2 Spike after BNT162b2 mRNA vaccination with a 16-week interval between doses. Cell Host Microbe *30*, 97–109.e5. https://doi.org/10.1016/j.chom.2021.12.004.

Tauzin, A., Gong, S.Y., Painter, M.M., Goel, R.R., Chatterjee, D., Beaudoin-Bussières, G., Marchitto, L., Boutin, M., Laumaea, A., Okeny, J., et al. (2022a). A Boost with SARS-CoV-2 BNT162b2 mRNA Vaccine Elicits Strong Humoral Responses Independently of the Interval between the First Two Doses. https://doi.org/10.1101/2022.04.18.22273967.

Tauzin, A., Nayrac, M., Benlarbi, M., Gong, S.Y., Gasser, R., Beaudoin-Bussières, G., Brassard, N., Laumaea, A., Vézina, D., Prévost, J., et al. (2021). A single dose of the SARS-CoV-2 vaccine BNT162b2 elicits Fc-mediated antibody effector functions and T cell responses. Cell Host Microbe *29*, 1137–1150.e6. https://doi.org/10.1016/j.chom.2021.06.001.

Tseng, H.F., Ackerson, B.K., Luo, Y., Sy, L.S., Talarico, C.A., Tian, Y., Bruxvoort, K.J., Tubert, J.E., Florea, A., Ku, J.H., et al. (2022). Effectiveness of mRNA-1273 against SARS-CoV-2 omicron and delta variants. Nat. Med. *28*, 1063–1071. https://doi.org/10.1038/s41591-022-01753-y.

ter Meulen, J., van den Brink, E.N., Poon, L.L.M., Marissen, W.E., Leung, C.S.W., Cox, F., Cheung, C.Y., Bakker, A.Q., Bogaards, J.A., van Deventer, E., et al. (2006). Human monoclonal antibody combination against SARS coronavirus: synergy and coverage of escape mutants. PLoS Med. *3*, e237. https://doi.org/10.1371/journal.pmed.0030237.

Ullah, I., Prévost, J., Ladinsky, M.S., Stone, H., Lu, M., Anand, S.P., Beaudoin-Bussières, G., Symmes, K., Benlarbi, M., Ding, S., et al. (2021). Live imaging of SARS-CoV-2 infection in mice reveals that neutralizing antibodies require Fc function for optimal efficacy. Immunity *54*, 2143–2158.e15. https://doi.org/10.1016/j.immuni.2021.08.015.

Yoon, S.K., Hegmann, K.T., Thiese, M.S., Burgess, J.L., Ellingson, K., Lutrick, K., Olsho, L.E.W., Edwards, L.J., Sokol, B., Caban-Martinez, A.J., et al. (2022). Protection with a third dose of mRNA vaccine against SARS-CoV-2 variants in frontline workers. N. Engl. J. Med. *386*, 1855–1857. https://doi.org/10.1056/NEJMc2201821.

STAR★METHODS

KEY RESOURCES TABLE

REAGENT or RESOURCE	SOURCE	IDENTIFIER
Antibodies		
LIVE-DEAD Fixable AquaVivid Cell Stain	Thermo Fischer Scientific	Cat# P34957
Mouse monoclonal anti-SARS-CoV-2 Spike (CR3022)	Dr M. Gordon Joyce (Meulen et al., 2006)	RRID: AB_2848080
CV3-25	(Jennewein et al., 2021)	N/A
Peroxidase AffiniPure Goat Anti-Human IgA + IgG + IgM (H + L)	Jackson ImmunoResearch	Cat # 109-035-064; RRID: AB_2337583
Goat anti-Human IgG Fc Cross-Adsorbed Secondary Antibody, HRP	Invitrogen	Cat # 31413; RRID: AB_429693
Alexa Fluor 647 AffiniPure Goat Anti-Human IgA + IgG + IgM (H + L)	Jackson ImmunoResearch	Cat # 109-605-064; RRID: AB_2337886
Cell Proliferation Dye eFluor 670	Thermo Fisher Scientific	Cat # 65-0840-85
Cell Proliferation Dye eFluor450	Thermo Fisher Scientific	Cat # 65-0842-85
Biological samples		
Health care workers blood samples	This paper	N/A
Solid organ transplant recipients blood samples	This paper	N/A
Chemicals, peptides, and recombinant proteins		
Dulbecco's Modified Eagle's medium (DMEM)	Wisent	Cat# 319-005-CL
Roswell Park Memorial Institute (RPMI)	Thermo Fischer Scientific	Cat# 61870036
Penicillin/Streptomycin	Wisent	Cat# 450-201-EL
Fetal Bovine Serum (FBS)	VWR	Cat# 97068-085
Bovine Serum Albumin (BSA)	Sigma	Cat# A7638
Phosphate Buffered Saline (PBS)	ThermoFischer Scientific	Cat# 10010023
Tween 20	Sigma	Cat# P9416-100ML
Puromycin Dihydrochloride	Millipore Sigma	Cat# P8833
Passive Lysis Buffer	Promega	Cat# E1941
Freestyle 293F expression medium	Thermo Fischer Scientific	Cat# A14525
D-Luciferin Potassium Salt	Thermo Fischer Scientific	Cat# L2916
Formaldehyde 37%	Thermo Fischer Scientific	Cat# F79-500
ExpiFectamine 293 transfection reagent	ThermoFisher Scientific	Cat# A14525
Western Lightning Plus-ECL, Enhanced Chemiluminescence Substrate	Perkin Elmer Life Sciences	Cat# NEL105001EA
Ni-NTA agarose	Invitrogen	Invitrogen
Experimental models: Cell lines		
HEK293T cells	ATCC	Cat# CRL-3216; RRID: CVCL_0063
293T-ACE2 cells	(Prévost et al., 2020)	N/A
FreeStyle 293F cells	ThermoFischer Scientific	Cat# R79007; RRID: CVCL_D603
CEM.NKr CCR5+ cells	NIH AIDS reagent program	Cat# ARP-4376; RRID:CVCL_X623
CEM.NKr CCR5+.S cells	(Anand et al., 2021)	N/A

(*Continued on next page*)

Continued

REAGENT or RESOURCE	SOURCE	IDENTIFIER
Recombinant DNA		
pNL4.3 R-E− Luc	NIH AIDS reagent program	Cat# 3418
pIRES2-EGFP	Clontech	Cat# 6029–1
pCG1-SARS-CoV-2 D614G-Spike	(Beaudoin-Bussières et al., 2020)	N/A
pCMV3-HCoV-HKU1-Spike	Sino Biological	Cat# VG40021-UT
pCAGGS-SARS-CoV-2-B.1.617.2-Spike (Delta)	(Gong et al., 2021)	N/A
pCAGGS-SARS-CoV-2-B.1.1.529-Spike (Omicron)	(Chatterjee et al., 2022)	N/A
Software and algorithms		
Flow Jo v10.7.1	Flow Jo	https://www.flowjo.com
GraphPad Prism v8.4.3	GraphPad	https://www.graphpad.com
R	R Core Team	http://www.R-project.org
Microsoft Excel v16	Microsoft Office	https://www.microsoft.com/en-ca/microsoft-365/excel
Other		
BD LSRII Flow Cytometer	BD Biosciences	N/A
TriStar LB942 Microplate Reader	Berthold Technologies	N/A

RESOURCE AVAILABILITY

Lead contact

Further information and requests for resources and reagents should be directed to and will be fulfilled by the lead contact, Andrés Finzi (andres.finzi@umontreal.ca).

Materials availability

All unique reagents generated during this study are available from the lead contact without restriction.

Data and code availability

- All data reported in this paper will be shared by the lead contact (andres.finzi@umontreal.ca) upon request.
- This paper does not report original code.
- Any additional information required to reanalyze the data reported in this paper is available from the lead contact (andres.finzi@umontreal.ca) upon request.

EXPERIMENTAL MODEL AND SUBJECT DETAILS

Ethics Statement

All work was conducted in accordance with the Declaration of Helsinki in terms of informed consent and approval by an appropriate institutional board. Blood samples were obtained from donors and recipients who consented to participate in this research project at Centre deRecherche du CHUM and approved by the CHUM Research Ethic board (19.381 and 21.001). Plasmas were isolated by centrifugation and Ficoll gradient, and samples stored at −80°C until use.

Human subjects

The study was conducted in 20 SARS-CoV-2 naïve vaccinated HCW (8 males and 12 females; age range: 33–64 years) and 64 SARS-CoV-2 vaccinated SOTR (39 males and 25 females; age range: 21–82 years). All this information is summarized in Table 1. For SARS-CoV-2 naïve vaccinated HCW cohort, no specific criteria such as number of patients (sample size), gender, clinical or demographic were used for inclusion, beyond no detection of Abs recognizing the N protein. For SARS-CoV-2 vaccinated SOTR, greater than 1-month post-transplant at the time of enrolment was used for inclusion and no detection of anti-N Abs at both time points.

Plasma and antibodies

Plasma from SOTR and HCW were collected, heat-inactivated for 1 hour at 56°C and stored at −80°C until ready to use in subsequent experiments. Plasma from uninfected donors collected before the pandemic were used as negative controls and used to calculate the seropositivity threshold in our ELISA, ADCC and flow cytometry assays (see below). The RBD-specific monoclonal antibody CR3022 was used as a positive control in our ELISA, and the CV3-25 antibody in flow cytometry assays and were previously described (Anand et al., 2020; Beaudoin-Bussières et al., 2020; Jennewein et al., 2021; Meulen et al., 2006; Prévost et al., 2020). Horseradish peroxidase (HRP)-conjugated Abs able to recognize the Fc region of human IgG (Invitrogen) were used as secondary Abs in ELISA experiments. Alexa Fluor-647-conjugated goat anti-human Abs able to detect all Ig isotypes (anti-human IgM+IgG+IgA; Jackson ImmunoResearch Laboratories) were used as secondary Abs to detect plasma binding in flow cytometry experiments.

Cell lines

293T human embryonic kidney cells (obtained from ATCC) were maintained at 37°C under 5% CO_2 in Dulbecco's modified Eagle's medium (DMEM) (Wisent) containing 5% fetal bovine serum (FBS) (VWR) and 100 μg/mL of penicillin-streptomycin (Wisent). CEM.NKr CCR5+ cells (NIH AIDS reagent program) and CEM.NKr.Spike cells were maintained at 37°C under 5% CO_2 in Roswell Park Memorial Institute (RPMI) 1640 medium (Gibco) containing 10% FBS and 100 μg/mL of penicillin-streptomycin. 293T-ACE2 cell line was previously reported (Prévost et al., 2020). CEM.NKr CCR5+ cells stably expressing the SARS-CoV-2 S glycoprotein were previously reported (Anand et al., 2021; Beaudoin-Bussières et al., 2021).

METHOD DETAILS

Plasmids

The HCoV-HKU1 S expressing plasmid was purchased from Sino Biological. The plasmids encoding the different SARS-CoV-2 Spike variants (D614G, Delta and Omicron) were previously described (Beaudoin-Bussières et al., 2020; Chatterjee et al., 2022; Gong et al., 2021; Tauzin et al., 2021,2022c). Briefly, for the D614G Spike, the single mutation was introduced using the QuikChange II XL site-directed mutagenesis protocol (Stratagene) in the pCG1-SARS-CoV-2-S plasmid kindly provided by Stefan Pöhlmann. Plasmids encoding Delta (B.1.617.2) and Omicron (B.1.1.529) Spikes were generated by overlapping PCR using a codon-optimized wild-type SARS-CoV-2 Spike gene (GeneArt, ThermoFisher) that was synthesized (Biobasic) and cloned in pCAGGS as a template. The presence of the desired mutations was determined by automated DNA sequencing.

Protein expression and purification

FreeStyle 293F cells (Invitrogen) were grown in FreeStyle 293F medium (Invitrogen) to a density of 1×10^6 cells/mL at 37°C with 8% CO_2 with regular agitation (150 rpm). Cells were transfected with a plasmid coding for SARS-CoV-2 S RBD (Beaudoin-Bussières et al., 2020) using ExpiFectamine 293 transfection reagent, as directed by the manufacturer (Invitrogen). One week later, cells were pelleted and discarded. Supernatants were filtered using a 0.22 μm filter (Thermo Fisher Scientific). The recombinant RBD proteins were purified by nickel affinity columns, as directed by the manufacturer (Invitrogen). The RBD preparations were dialyzed against phosphate-buffered saline (PBS) and stored in aliquots at −80°C until further use. To assess purity, recombinant proteins were loaded on SDS-PAGE gels and stained with Coomassie Blue.

Enzyme-linked immunosorbent assay (ELISA) and RBD avidity index

The SARS-CoV-2 RBD ELISA assay used was previously described (Beaudoin-Bussières et al., 2020; Prévost et al., 2020). Briefly, recombinant SARS-CoV-2 S RBD proteins (2.5 μg/mL) were prepared in PBS and were adsorbed to plates (MaxiSorp Nunc) overnight at 4°C. Coated wells were subsequently blocked with blocking buffer (Tris-buffered saline [TBS] containing 0.1% Tween20 and 2% BSA) for 1h at room temperature. Wells were then washed four times with washing buffer (Tris-buffered saline [TBS] containing 0.1% Tween20). CR3022 mAb (50 ng/mL) or a 1/250 dilution of plasma were prepared in a diluted solution of blocking buffer (0.1% BSA) and incubated with the RBD-coated wells for 90 min at room temperature. Plates were washed four times with washing buffer followed by incubation with secondary Abs (diluted in a solution of blocking buffer (0.4% BSA)) for 1h at room temperature, followed by four washes. To calculate the RBD-avidity index, we performed in parallel a stringent ELISA, with same steps than for the ELISA assay but where the plates were washed with a chaotropic agent, 8M of urea, added of the washing buffer. This assay was previously described (Tauzin et al., 2022b). For both assays, HRP enzyme activity was

determined after the addition of a 1:1 mix of Western Lightning oxidizing and luminol reagents (Perkin Elmer Life Sciences). Light emission was measured with a LB942 TriStar luminometer (Berthold Technologies). Signal obtained with BSA was subtracted for each plasma and was then normalized to the signal obtained with CR3022 present in each plate. The seropositivity threshold was established using the following formula: mean of pre-pandemic SARS-CoV-2 negative plasma + (3 standard deviation of the mean of pre-pandemic SARS-CoV-2 negative plasma). The RBD avidity index was calculated using the formula: RBD avidity index = ((level of anti-RBD IgG measured with urea)/(level of anti-RBD IgG measured without urea))×100.

Cell surface staining and flow cytometry analysis

293T cells were co-transfected with a GFP expressor (pIRES2-GFP, Clontech) in combination with plasmid encoding the full-length S of SARS-CoV-2 variants (D614G, Delta or Omicron) or the HCoV-HKU1 S. 48h post-transfection, S-expressing cells were stained with the CV3-25 Ab (Jennewein et al., 2021) or plasma (1/250 dilution). Alexa Fluor-647-conjugated goat anti-human IgM+IgG+IgA Abs (1/800 dilution) were used as secondary Abs. The percentage of transfected cells (GFP + cells) was determined by gating the living cell population based on viability dye staining (Aqua Vivid, Invitrogen). Samples were acquired on a LSRII cytometer (BD Biosciences), and data analysis was performed using FlowJo v10.7.1 (Tree Star). The seropositivity threshold was established using the following formula: (mean of pre-pandemic SARS-CoV-2 negative plasma + (3 standard deviation of the mean of pre-pandemic SARS-CoV-2 negative plasma). The conformational-independent S2-targeting mAb CV3-25 was used to normalize Spike expression and was shown to effectively recognize all SARS-CoV-2 Spike variants (Li et al., 2022).

ADCC assay

This assay was previously described (Anand et al., 2021; Beaudoin-Bussières et al., 2021). Briefly, for evaluation of anti-SARS-CoV-2 ADCC, parental CEM.NKr CCR5+ cells were mixed at a 1:1 ratio with CEM.NKr cells stably expressing a GFP-tagged full length SARS-CoV-2 Spike (CEM.NKr.SARS-CoV-2.Spike cells). These cells were stained for viability (AquaVivid; Thermo Fisher Scientific, Waltham, MA, USA) and cellular dyes (cell proliferation dye eFluor670; Thermo Fisher Scientific) to be used as target cells. Overnight rested PBMCs were stained with another cellular marker (cell proliferation dye eFluor450; Thermo Fisher Scientific) and used as effector cells. Stained target and effector cells were mixed at a ratio of 1:10 in 96-well V-bottom plates. Plasma (1/500 dilution) were added to the appropriate wells. The plates were subsequently centrifuged for 1minat 300g, and incubated at 37°C, 5% CO_2 for 5 hours before being fixed in a 2% PBS-formaldehyde solution. ADCC activity was calculated using the formula: [(% of GFP + cells in Targets plus Effectors)-(% of GFP + cells in Targets plus Effectors plus plasma/antibody)]/(% of GFP + cells in Targets) x 100 by gating on transduced live target cells. All samples were acquired on an LSRII cytometer (BD Biosciences) and data analysis was performed using FlowJo v10.7.1 (Tree Star). The specificity threshold was established using the following formula: (mean of pre-pandemic SARS-CoV-2 negative plasma + (3 standard deviation of the mean of pre-pandemic SARS-CoV-2 negative plasma).

Virus neutralization assay

To produce the pseudoviruses, 293T cells were transfected with the lentiviral vector pNL4.3 R-E− Luc (NIH AIDS Reagent Program) and a plasmid encoding for the indicated S glycoprotein (D614G, Delta or Omicron) at a ratio of 10:1. Two days post-transfection, cell supernatants were harvested and stored at −80°C until use. For the neutralization assay, 293T-ACE2 target cells were seeded at a density of 1×10^4 cells/well in 96-well luminometer-compatible tissue culture plates (Perkin Elmer) 24h before infection. Pseudoviral particles were incubated with several plasma dilutions (1/50; 1/250; 1/1250; 1/6250; 1/31250) for 1h at 37°C and were then added to the target cells followed by incubation for 48 hat 37°C. Then, cells were lysed by the addition of 30 μL of passive lysis buffer (Promega) followed by one freeze-thaw cycle. An LB942 TriStar luminometer (Berthold Technologies) was used to measure the luciferase activity of each well after the addition of 100 μL of luciferin buffer (15mM $MgSO_4$, 15mM KPO_4 [pH 7.8], 1mM ATP, and 1mM dithiothreitol) and 50 μL of 1mM d-luciferin potassium salt (Prolume). The neutralization half-maximal inhibitory dilution (ID_{50}) represents the plasma dilution to inhibit 50% of the infection of 293T-ACE2 cells by pseudoviruses.

QUANTIFICATION AND STATISTICAL ANALYSIS

Statistical analysis

Symbols represent biologically independent samples from SOTR and HCW. Lines connect data from the same donor. Statistics were analyzed using GraphPad Prism version 8.0.1 (GraphPad, San Diego, CA). Every dataset was tested for statistical normality and this information was used to apply the appropriate (parametric or nonparametric) statistical test. Differences in responses for the same donor after the second and third dose of mRNA vaccine were performed using Mann-Whitney tests. Differences in responses between HCW and SOTR at D2 or D3 were measured by Kruskal-Wallis tests. p values <0.05 were considered significant; significance values are indicated as * $p < 0.05$, ** $p < 0.01$, *** $p < 0.001$, **** $p < 0.0001$. Spearman's R correlation coefficient was applied for correlations. Statistical tests were two-sided and $p < 0.05$ was considered significant.

Software scripts and visualization

Edge bundling graphs were generated in undirected mode in R and RStudio using ggraph, igraph, tidyverse, and RColorBrewer packages (R Core Team, 2014). Edges are only shown if $p < 0.05$, and nodes are sized according to the connecting edges' r values. Nodes are color-coded according to groups of variables.